Acta Mechanica Slovaca **27 (3): 54 - 61,** September **2023**
https://doi.org/10.21496/ams.2023.031

Acta Mechanica Slovaca
ISSN 1335-2393
www.actamechanica.sk

Formability Evaluation and Strain Distribution at the Limit Dome Height Test of Dual-Phase Steel

Miroslav Tomáš [1*], Juliy Martyn Kulya [1], Vladimír Kokarda [2]

[1] Department of Automotive Production, Faculty of Mechanical Engineering, Technical University of Kosice, Slovakia

[2] Carl Zeiss Slovakia, s.r.o - ZEISS Industrial Quality Solutions, Bratislava, Slovakia

Abstract: The article deals with the formability testing of dual-phase steel DP800 that is used for the production of parts used in the rear deformation zone of the car body. The thickness of the steel was 1.6mm, and the Limit Dome Height test was performed on an Erichsen 145-60 testing machine. Specimens of different widths were stretched up to the fracture, and the punch path and force were measured. Specimens were etched to create a deformation grid of dots in order to measure the strain distribution using the photogrammetric system Argus. Then, the simulation model of the LDH test was created, and the punch path was set to calculate the strain distribution when constitutive equations Hill 48 and the Hollomon model described the material. The results of strain distribution measured experimentally were compared to those numerically simulated using both explicit and implicit simulation software. Limit Dome Height (LDH=23.5±1.5mm) was reached for specimen 108 mm, and measurements of strain distribution confirmed the plain strain state. A better description of principal strain distribution was reached at numerical simulation by the implicit simulation software, where the relative error of both the maximum stretching force and principal strains was lower.

Keywords: LDH test, Stretching force, Punch path, Experiment, Simulation, Relative error

Introduction

Demands of making cars lighter weight to achieve lower emissions during their operation, but still keeping passengers safety, steel grades like AHSS are implemented in the body structure. These steels offer using lower steel sheets thickness for stamped part due to their higher strength. Dual-phase steels are commonly used in certain car-body parts because of their good combination of strength and ductility and low production costs [1].

Formability, defined as the ability of sheet metal to be stamped without any fracture, depends on several interacting factors [2]. The total formability can be classified as a material one and process one [3]. Material formability can be easily tested by the tests which lies on simple tensile or compression test. Otherwise, process formability includes several process-depending factors when combined with material properties. Due to different stress-strain distribution in each stamped part region, there is no single testing procedure for satisfying to test formability in a simple way. Thus, different simulative tests are used, such as Erichsen, Engelhardt, Cup test, Limit Dome height etc. [2-5].

Limit dome height test (LDH), introduced by Ghosh and modified by Hecker, was developed to simulate the fracture conditions under plane-strain deformation, which was identified by the Hecker as more than 80% of the stamping failures [6,7].

*** Corresponding author:** Miroslav Tomáš, ***E-mail address:*** *miroslav.tomas@tuke.sk*

Table 1: Mechanical properties of dual-phase steel DP800, thickness 1.6 mm.

Rolling direction	Rp0.2 [MPa]	Rm [MPa]	A80 [%]	r [–]	rm [–]	n [–]	nm [–]	K [MPa]
0°	527	828	19.9	0.873		0.126		1219
45°	508	830	18.2	0.907	0.917	0.125	0.125	1223
90°	496	838	18.4	0.979		0.123		1229

Note: Rp0.2–yield strength, Rm–tensile strength, A80–elongation, r–plastic strain ratio, rm–mean value of plastic strain ratio, n–strain hardening exponent, nm–mean value of strain hardening exponent, K–material constant

Furthermore, the test was modified to use metal sheet strips with different width, material thickness and laser welded dissimilar materials. Sahu [8] applied LDH test to study deformation properties of very thin brass sheet. They modelled biaxial, plane-strain and uniaxial strain paths by scaling down the tool and specimen dimensions and evaluated limit strains as well. Xie and Nakamachi [9] predicted the formability of high-strength steels and by using elastic/crystalline viscoplastic FE analyses of standard LDH tests. From LDH formability test they confirmed that the combination of high-strength steel with a little proportion of gama texture components could lead to significant improvement of formability. Kuramae et al. [10] performed modified LDH test on four automotive sheet-metals: aluminum alloy sheet-metals A6022-T43, A5182-O, A6022-ASR (an asymmetrically rolled), and mild-steel HC220YD. They performed formability analysis from the view of microcrystalline texture evolution during plastic deformation by the multi-scale LDH test analysis, which was done by using multiscale parallel finite element procedure. As a result, they compared the results of FE prediction of fracture to the LDH test performed with flat head punch for various strain path conditions. Katragadda et al. [11] conducted LDH test for different steel grades used in automotive industry. Results of experiments compared to the simulations when applied Hill 48 and Hollomon's equation as constitutive equations to describe material behavior. Bandyopadhyay et al. [12] conducted formability tests for laser welded tailor welded blanks of dissimilar materials (DP980/DP600 and DP980/IFHS). They found out the decrease of formability for LDH and Erichsen cupping test were approximately following similar trend, and hence, the punch size played a minor influence.

The aim of the article is to evaluate the formability of dual-phase steel DP800 and the accuracy of the applied simulation model in forecasting this formability by comparing the results. Otherwise, principal strains will be measured by the photogrammetric system Argus and compared to the strains calculated in the explicit and implicit simulation software for the volume blank.

2 Materials and Methods

2.1 Experimental material

Formability of dual-phase high strength steel DP800 with thickness 1.6mm was assessed by the LDH test. Mechanical properties of experimental material were tested according to standard: ISO 6892-1, plastic strain ratio according to ISO 10113 and strain hardening exponent according to ISO 10275. Samples for mechanical tests were taken in rolling direction 0°, 45° and 90° to describe material anisotropy. Three specimens were measured in each direction and average values are shown in Table 1. Tests were performed on TIRA test 2300 testing machine equipped with longitudinal and transversal extensometers with precision 0.001 mm. The plastic strain ratio was evaluated at uniform elongation level 12% and the strain hardening exponent within the range 5% to uniform elongation.

2.2 Limit Dome Height Test

The LDH test was used to determine the formability of sheet metals at different minor to major strain ratios by evaluation the dome height and it is comparable to a Nakajima test. A hemispherical punch stretches the clamped specimen until fracture. Experiments were conducted on Erichsen 145-60 testing machine with Nakajima tooling setup. Testing sequences were automatically controlled and machine control unit had controlled and recorded the punch path, blank holding force and stretching force. During experiments blanks width of 196, 133, 108, 70, 39 and 26 millimeters were tested as it is shown in Fig.1. PTFE foil with thickness 0.2mm was used as a lubricant.

Figure 1: Types of blanks.

2.3 Strain evaluation by Argus

The deformation grid was applied to the samples by electrochemical etching using an ÖSTLING EU Classic 300 device. Rectangular deformation grid consisted of dots with diameter 1mm and spacing 2 mm in rows and columns. The Argus 3D optical system from the German company GOM was used to measure the applied deformation mesh – Fig. 2. Besides of other method to evaluate strain distribution [13], etched grid and optical system is a well-established and frequently used device for the evaluation of various types of forming processes due to its complexity [14,15,16].

Series of photo was taken by 12Mpix digital camera Nikon 300D from 3 different height positions with 12 positions in each height level. Then, based on coded points and calibrated bars positioned around the specimen, software evaluated the position of each point and calculated the deformation grid. Limit strains, major and minor, were evaluated as mean average value from five points located nearest to the top of the dome (for specimens 26, 108 and 196mm) and nearest to the fracture – Fig. 3.

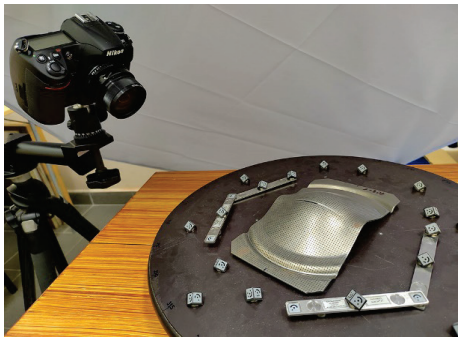

Figure 2: Photogrammetric system Argus.

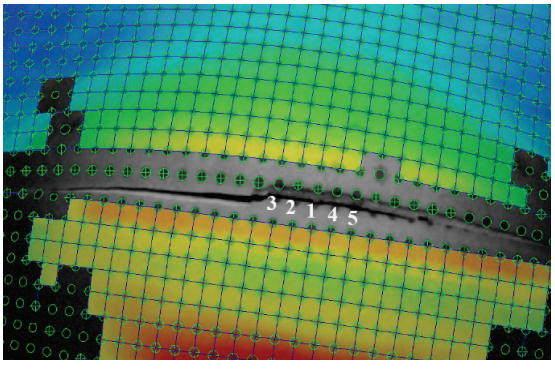

Figure 3: Points taken for strain evaluation (specimen 108 mm).

2.4 Simulation model of LDH test

The simulation model of LDH test, as it is shown in Fig. 4, consisted of three parts – die (green), punch (red), blank holder (turquoise), and blank (purple). The dimensions were as specified for Nakajima test: punch diameter 100mm, die diameter 106mm, die radius R12. Simulation was performed in both, the explicit and the implicit simulation software for volume blank when locking by restriction bead (as a part of blank holder and die) and blank holder force set to 300kN. Simulation was set as 3D and volume blanks were meshed as solid finite elements with size 2mm (implicit software) and 2x2mm 7 layers (explicit software). Friction was set as a Coulomb's with the value 0.02. Simulations were performed for maximum and minimum punch path reached at the experiments for specimen width 26, 108 and 196mm.

Material constitutive equations, yield law and hardening curve were defined as follows: [2,15,17]

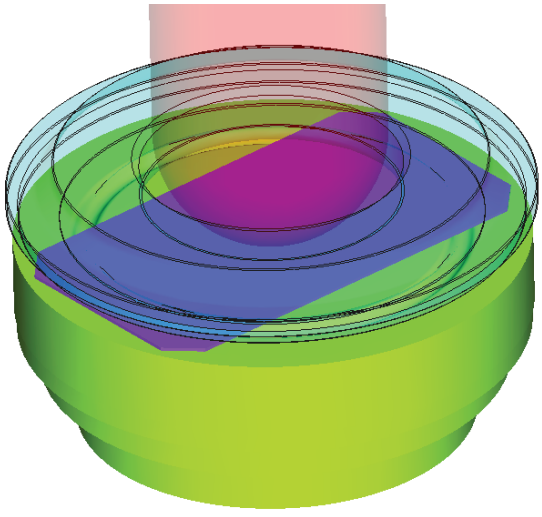

Figure 4: Simulation model of the LDH test.

Hill 48 anisotropic plasticity model:

$$\sigma_1^2 + \frac{r_0\left(1+r_{90}\right)}{r_{90}\left(1+r_0\right)}\sigma_2^2 - \frac{2r_0}{1+r_0}\sigma_1\sigma_2 = \left(\sigma_1^y\right) \qquad (1)$$

where σ_1, σ_2 are principal stresses; σ_1^y is the yield stress and r_0, r_{45}, r_{90} are plastic strain ratios (Lankford's coefficients) in specified rolling direction.Hollomon hardening model (Eq. 2).

$$\sigma = K \cdot \varphi^n \qquad (2)$$

where K is material constant, n is strain hardening exponent.

3. Results and Discussion

The results of the maximum stretching force and the punch path up to the specimen fracture for the individual width of the samples are given in Table 2. Three measurements for each width were carried out and the average value of the maximum force at fracture were calculated. Fig.5 shows a comparison of the achieved punch path for each specimen width. The minimum value of punch path – LDH parameter – was recorded for a specimen width of 108mm, thus parameter LDH=23.5±1.5mm. The results comply to the results of Takahashi, which performed the LDH test on AHSS steel and the minimum dome height was reached for the plain-strain state [18,19].

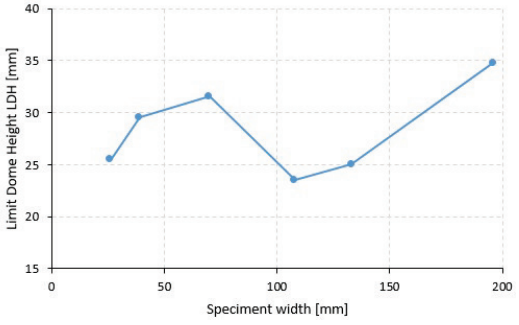

Figure 5: LDH test result: dependence of the dome height at fracture on the blank width.

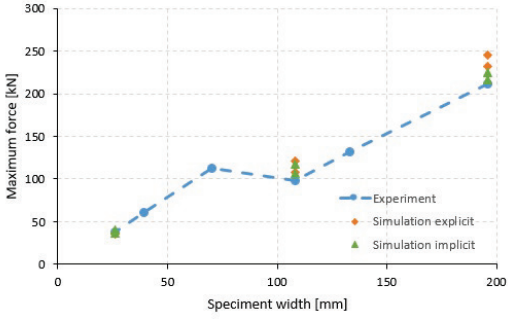

Figure 6: LDH test results: dependence of the maximum force on the blank width and comparison to the results from numerical simulation.

Partial results of the LDH test numerical simulation for specimen width 26, 108 and 196 mm are shown in the Table 2 also. They are compared to the experimental results in the Fig. 6 and the relative error was calculated as follows:

$$\delta\left(X\right) = X_{simulation} - X_{experiment} \qquad (3)$$

where X is the value (the maximum stretch force, major or minor strain later), Xsimulation is the value evaluated in numerical simulation and Xexperiment is the average value evaluated in experiment.

As it is shown in Table 2, there was found very small difference of maximum stretching force for specimen width 26mm with value of -2.40kN to -1.16kN (explicit software); or -0.32kN to 2.56kN (implicit software), when the first value is for the minimum and the second value is for the maximum of punch path reached at experiment. When specimen width arose to 108mm, the difference in maximum stretching force arose as well with the value of 9.38kN to 23.37kN (explicit software); or 8.78kN to 19.31kN (implicit software).

Table 2: Measured and calculated values of the maximum force and the punch path at fracture.

Blank width	Experiment			Simulation		Relative error	
				explicit	implicit	explicit	implicit
	Fmax [kN]		Stroke [mm]	Fmax [kN]	Fmax [kN]	δ(Fmax,expl [kN]	δ(Fmax,impl [kN]
	measured	average					
196	211.31 205.68 217.22 211.40	211.4	34.44 33.16 36.62	231.61 245.25	216.12 224.71	20.20 33.84	4.71 13.30
133	133.88 127.39 132.75	131.3	25.40 24.54 25.16				
108	97.53 92.67 103.76	97.9	23.40 22.52 24.58	107.37 121.36	106.77 117.30	9.38 23.37	8.78 19.31
070	110.11 114.52	112.3	30.86 32.28				
039	60.45 61.29 58.86	60.2	29.42 30.16 28.98				
026	37.91 37.37 37.36	37.5	26.16 24.46	36.39 35.15	40.11 37.23	-1.16 -2.40	2.56 -0.32

Table 3: Results of principal strains evaluated by Argus and calculated by numerical simulation.

Blank width [mm]	Punch path	Experiment		Simulation explicit		Simulation implicit	
		f1 [–]	f2 [–]	f1 [–]	f2 [–]	f1 [–]	f2 [–]
196	Min Max	0.369 –	0.337 –	0.383 0.464	0.276 0.313	0.394 0.478	0.378 0.459
108	Min Max	0.218 –	0.007 –	0.240 0.306	0.034 0.031	0.154 0.221	0.042 0.045
26	Min Max	0.352 –	-0.145 –	0.260 0.328	-0.083 -0.107	0.250 0.339	-0.082 -0.108

Note: φ1 – major strain; φ2 – minor strain

Table 4: Relative error of the numerical simulation when compared to the experiment results.

Blank width [mm]	Punch path	Simulation explicit		Simulation implicit	
		δ(φ1) [–]	δ(φ2) [–]	δ(φ1) [–]	δ(φ2) [–]
196	Min Max	0.014 0.095	-0.061 -0.024	0.025 0.109	0.041 0.122
108	Min Max	0.022 0.088	0.027 0.024	-0.064 0.003	0.035 0.038
26	Min Max	-0.092 -0.024	0.062 0.038	-0.102 -0.013	0.063 0.037

Note: φ1 – major strain; φ2 – minor strain

Maximum difference in forces was found for specimen width of 198mm with value of 20.20kN to 33.84kN (explicit software); or 4.71kN to 13.30kN (implicit software). It can be stated that the implicit software gave smaller difference of maximum stretch force when compared to the experimental results.

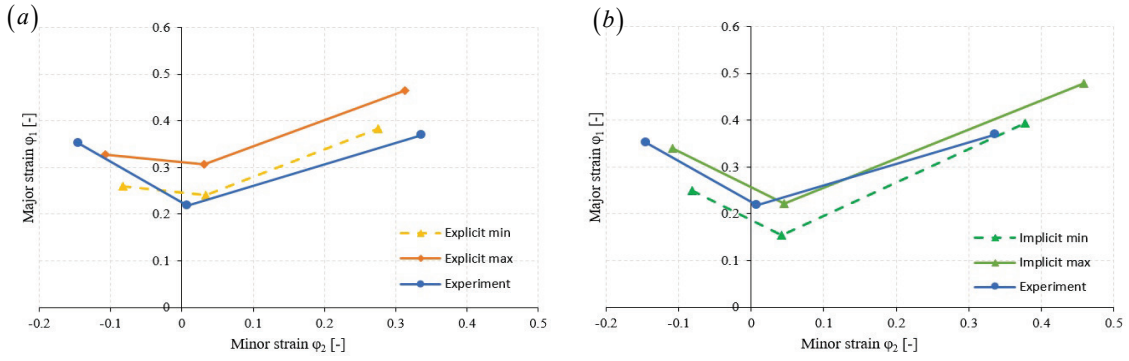

Figure 7: Comparison of the principal strains measured using Argus and calculated by numerical simulation for explicit (a) and implicit (b) simulation software.

The results of the strain distribution measured by the Argus system and determined by numerical simulations are given in Tab.3. Calculated relative error of numerical simulation for explicit and implicit software is shown in Tab. 4. The graphical comparison is shown in Fig. 7a for the explicit and in Fig. 7b for the implicit simulation software. When evaluate results of numerical simulation for explicit simulation software, it can be seen the major strain is underestimated for $\varphi_2<0$ with relative error -0.024 to -0.092, and overestimated for $\varphi_2>0$ with relative error 0.014 to 0.095. It is also important to notice that relative error of minor strain for specimen 26mm, i.e. $\varphi_2<0$ is negative, and relative error of minor strain for specimen 196mm, i.e. $\varphi_2>0$ is positive. The relative error for specimen 108 mm, i.e. $\varphi_2\approx0$ is positive as well. When evaluate results of numerical simulation for implicit simulation software, it can be seen the major strain is underestimated for $\varphi_2<0$ with relative error -0.013 to -0.102, and overestimated for $\varphi_2>0$

Table 5: Comparison of the principal strains measured experimentally and calculated by numerical simulation for specimen 108mm (implicit software).

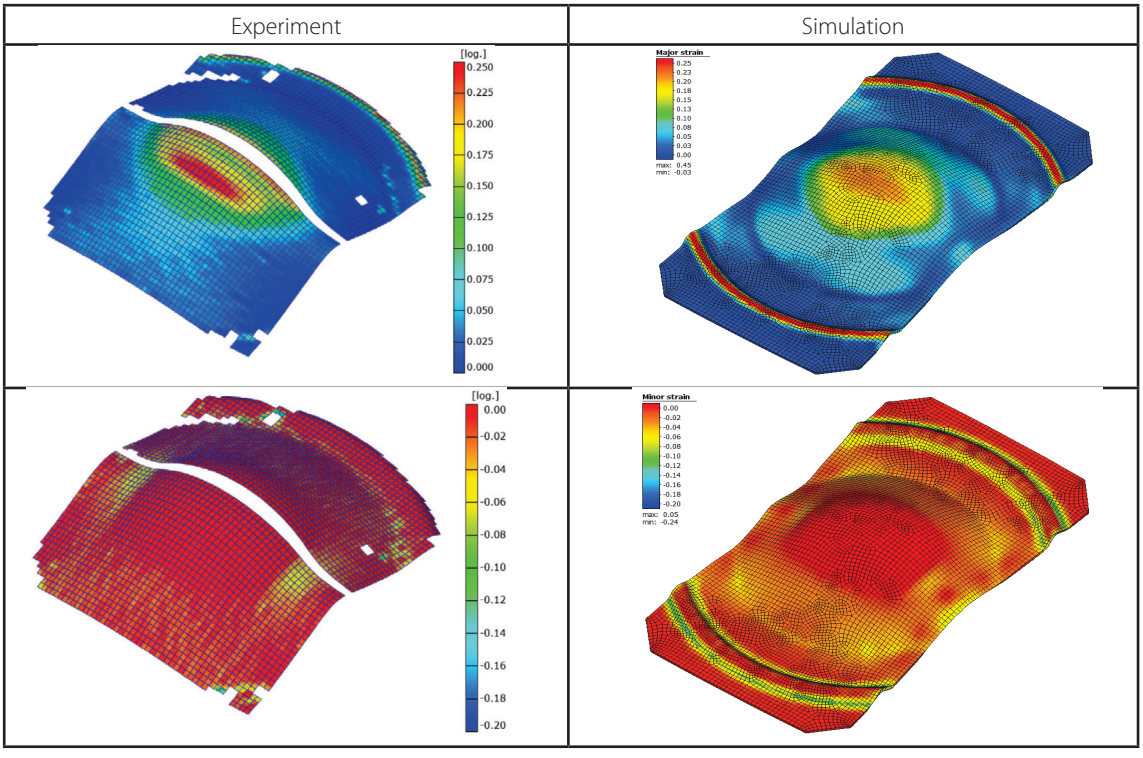

with relative error 0.025 to 0.109. But, the relative error of minor strains for $\varphi_2<0$, $\varphi_2\approx0$, and $\varphi_2>0$ have the same direction. Thus, the whole curve is positioned right to the experimentally measured one. It might be caused by the friction definition in simulation software, which is considered constant.

Considering the relative error of the stretch force, the relative error of the principal strains, and the position of curves in Fig. 7 it is supposed better description of strain distribution for implicit simulation software. The difference between experimental and simulation results might be caused by the measurement error and other factors [14,15,16]. Major strains of the fracture zone when measured by Argus were significantly larger than those of the safety zone [20]. Even though the results of numerical simulations depend on yield law-hardening law combination, it is possible to state a good agreement between the results of experimental measurements and numerical simulation [21,22].

4. Conclusions

The article presents the result of the LDH test conducted on the dual-phase steel DP800. This steel is being used to make stamped parts for the rear deformation zone of cars. The minimal punch path, i.e., the LDH parameter, was reached for the plane-strain condition modeled by specimen width 108 mm. It was confirmed by measuring the strain distribution using the ARGUS photogrammetric system. The results of strain distribution for selected samples were also correlated to the numerical simulation of the LDH test using explicit and implicit simulation software. Comparing the results of maximum stretch force and principal strains in experiments and numerical simulations, it can be stated:

– explicit and implicit simulation software overestimated the maximum stretching force, but the implicit software gave a smaller relative error of the maximum stretch force when compared to the experimental results;

– the principal strain distribution for specimen 26 mm was underestimated by the explicit simulation for both, the maximum and minimum punch paths, while the principal strains for 108 mm and 196 mm were overestimated;

– the principal strain distribution calculated by implicit simulation software gave a better description of strain distribution, considering the position of the curves, when the principal strains were slightly underestimated for 26mm and 108mm specimens and overestimated for 196 mm specimen.

Further research will be focused on the evaluation of limit strains and their correlation to the numerical simulation.

Acknowledgments: The work was done under the grant project VEGA 1/0238/23 "Implementation of CAx systems and virtual engineering techniques in the redesign of car-body parts for deformation zones".

References

[1] Oliver S., Jones T.B., Fourlaris G. (2007). Dual phase versus TRIP strip steels: Microstructural changes as a consequence of quasi-static and dynamic tensile testing. Materials Characterization, Vol. 58, p. 390-400.

[2] Hrivňák A., Evin E. (2004). Formability of metal sheets, 1st ed.; Košice : Technical University, Slovakia, pp. 223.

[3] Mielnik E.M. (1991). Metalworking Science and Engineering, McGraw-Hill, p. 976.

[4] Hosford W.F., Caddell R.M. (2012), Metal Forming, Mechanics and Metallurgy, 3rd edition, Cambridge University Press.

[5] Čada R. (1997). Formability of Deep-Drawing Steel Sheets. Proceedings of the 5th European Conference on Advanced Materials and Processes and Applications (EUROMAT 97): Materials, Functionality Design: Volume 4 - Characterization and Production/Design., p. 463-466.

[6] Narasimhan K., Miles M.P., Wagoner R.H. (1995). A better sheet-formability test, Journal of Materials Processing Technology, Volume 50, p. 385-394.

[7] ASM Handbook (1988), Forming and Forging, ASM International, 9th Edition Metals Handbook.

[8] Sahu J., Mishra S. (2016). Limit dome height test of very thin brass sheet considering the scaling effect. Journal of Physics Conference Series, Vol. 734, p. 1-4.

[9] Xie C.L., Nakamachi E. (2002). The effect of crystallographic textures on the formability of high-strength steel sheets. Journal of Materials Processing Technology, Vol. 122, p. 104-111.

[10] Kuramae H., Ikeya Y., Sakamoto H., Morimoto H., Nakamachi E. (2010). Multi-scale parallel finite element analyses of LDH sheet formability tests based on crystallographic homogenization method. International Journal of Mechanical Sciences, Vol. 52, p. 183-197.

[11] Katragadda S.C., Ramulu P. (2014). Investigation of forming behavior prediction of different steel grade materials using numerical simulation. 5th International & 26th All India Manufacturing Technology, Design and Research Conference, India.

[12] Bandyopadhyay K., Panda S.K., Saha P., Padmanabham G. (2015). Limiting drawing ratio and deep drawing behavior of dual phase steel tailor welded blanks: FE simulation and

experimental validation. Journal of Materials Processing Technology, Vol. 217, p. 48-64.

[13] Čada, R. (2003). Testing of Strain in Stampings by Embossed Grids. Technical Gazette, Vol. 10, No. 3-4, pp. 9-13.

[14] Slota J., Jurčišin M, Gajdoš I., Spišák E. (2013). The sensitivity of a photogrammetric method in formability analysis. Acta Mechanica et Automatica, Vol. 7(2), p. 117-123.

[15] Fracz W., Stachowicz F., Pieja T. (2013). Aspects of verification and optimization of sheet metal numerical simulations process using the photogrammetric system. Acta Metallurgica Slovaca, Vol. 19(1), p, 51-59.

[16] Duchac A., Kejzlar P. (2023). Optimization of Raster Point Deposition Methodology for Deformation Analyses. Materials Science Forum, Vol. 1081, p.155-160.

[17] Čada R., Pektor T. (2022). Design of Stamping Drawing Technology from Thin Sheet. Proceedings of the 31st International Conference on Metallurgy and Materials METAL 2022. 1st ed., Brno: Tanger, s.r.o., p. 262-267.

[18] AHSS Guidelines, Available online: https://www.worldautosteel.org/projects/advanced-high-strength-steel-application-guidelines/.

[19] Takahashi M. (July 2003). Development of High Strength Steels for Automobiles, Nippon Steel Technical Report No. 88.

[20] Sun L., Cai Z., He D.; Li L. (2019). Aluminum Alloy Sheet-Forming Limit Curve Prediction Based on Original Measured Stress–Strain Data and Its Application in Stretch-Forming Process. Metals, 9(10): 1129.

[21] Tomáš M., Ižol P. (2016). Assessment of deep-drawing process by photogrammetric method when design the tin car body production. Transfer inovacií, Vol. 33, p. 104-107.

[22] Mulidrán P., Šiser M., Slota J., Spišák E., Sleziak T. (2018). Numerical Prediction of Forming Car Body Parts with Emphasis on Springback. Metals, 8(6): 435.